Altered calmodulin degradation and signaling in non-neuronal cells from Alzheimer's disease patients.

Noemí Esteras[1], Úrsula Muñoz[1,5], Carolina Alquézar[1], Fernando Bartolomé[1], Félix Bermejo-Pareja[2,3] , and Ángeles Martín-Requero[1,4]

[1]Department of Cellular and Molecular Medicine. Centro de Investigaciones Biológicas (CSIC), Ramiro de Maeztu 9, 28040 Madrid, Spain [2]Hospital Doce de Octubre, Avda. de Córdoba s/n, 28041 Madrid, [3]Centro de Investigación Biomédica en Red de Enfermedades Neurodegenerativas (CIBERNED), [4]Centro de Investigación Biomédica en Red de Enfermedades Raras (CIBERER), [5]Present address: Mount Sinai School of Medicine, 1425 Madison Avenue, New York, NY 10029, USA

Running title: Impaired calmodulin degradation in AD cells.

Key words: Alzheimer's disease, Ca^{2+}/Calmodulin, CaMKII, lymphocytes, PI3K/Akt, ROS

Address for correspondence:

Dr. Ángeles Martín-Requero

Centro de Investigaciones Biológicas (CSIC)

Ramiro de Maeztu 9

28040 Madrid, SPAIN

Phone: 34-91-837-3112

Fax: 34-91-536-0432

E-mail: amrequero@cib.csic.es

ABSTRACT

Previous work indicated that changes in Ca^{2+}/calmodulin (CaM) signaling pathway are involved in the control of proliferation and survival of immortalized lymphocytes from Alzheimer's disease (AD) patients. We examined the regulation of cellular CaM levels in AD lymphoblasts. An elevated CaM content in AD cells was found when compared with control cells from age-matched individuals. We did not find significant differences in the expression of the three genes that encode CaM: CALM1, 2, 3, by real time RT-PCR. However, we observed that the half-life of CaM was higher in lymphoblasts from AD than in control cells, suggesting that degradation of CaM is impaired in AD lymphoblasts. The rate of CaM degradation was found to be dependent on cellular Ca^{2+} and ROS levels. CaM degradation occurs mainly via the ubiquitin-proteasome system. Increased levels of CaM were associated with overactivation of PI3K/Akt and CaMKII. Our results suggest that increased levels of CaM synergize with serum to overactivate PI3K/Akt in AD cells by direct binding of CaM to the regulatory α-subunit (p85) of PI3K. The systemic failure of CaM degradation, and thus of Ca^{2+}/CaM-dependent signaling pathways, may be important in the etiopathogenesis of AD.

INTRODUCTION

Dysregulation of calcium homeostasis is among the major cellular alterations in Alzheimer's disease, leading to neuronal dysfunction and ultimately apoptosis [1-3]. As the major cellular Ca^{2+}-binding protein, CaM responds to calcium fluxes by binding and regulating the activity of multiple CaM-dependent proteins [4]. Some of these CaM-binding proteins (CaMBPs) are involved in fundamental events of calcium-mediated neuronal function, as well as in processes such as learning and memory [5]. Moreover, a search for CaMBPs revealed that many of the proteins intimately linked to AD, such as tau or presenilins, may be calmodulin-binding proteins [5]. CaM consists of two homologous domains (N- and C-terminal), and each domain contains two EF-hand Ca^{2+}-binding motifs [6, 7]. Apo-CaM forms a closed conformation by its two homologous domains. Once Ca^{2+} binds to the EF-hand motifs in both domains, the conformation of CaM changes into an open form, allowing for its client proteins to access hydrophobic pockets located in the inner parts of each domain [8, 9]. Consequently, the protein is implicated in a variety of cellular functions, and most importantly CaM levels change with age [10].

Since the concentration of CaM-dependent target proteins exceeds that of cellular CaM, changes in rates of CaM expression and/or degradation will have important physiological effects on the availability of CaM for target protein regulation [11, 12]. In particular, during biological aging, the cellular abundance of CaM is altered, and oxidized fragments accumulate. Underlying these age-dependent changes in CaM abundance may be oxidant-induced structural changes that promote the recognition and degradation of CaM [10].

On the other hand, alterations in calcium signaling are not restricted to neuronal cells. They also have been reported for peripheral cells such as fibroblasts and lymphocytes, which represent easy to obtain diagnostic material [13-15]. Changes in CaM availability and/or in the intrinsic functional properties of the molecule were linked to disruption of Ca^{2+} homeostasis in immortalized lymphocytes from late-onset AD patients [14]. Interestingly, the distinct Ca^{2+} response of AD was associated with enhanced cell proliferation compared to control lymphoblasts from age-matched individuals [16, 17]. These features were considered as peripheral signs of the disease, as current evidence relates the process of neuronal apoptosis occurring in AD to the aberrant reentry of differentiated neurons into the cell cycle [18-20].

The source of signals that drive cell division in the neurons of AD patients is not yet known. Since CaM has long been implicated in the regulation of cell proliferation [21, 22], and alterations in CaM content and activity have been reported in AD brain [23, 24], the possibility that this molecule could play a

significant role in the cell cycle-mediated neurodegeneration in AD should be considered.

We previously reported that Ca^{2+}/CaM stimulates proliferation and increases resistance to serum deprivation-mediated cell death in lymphoblasts from AD patients. [16, 17, 25, 26]. It was proposed that there is a functional relationship between $Ca^{2+/}$CaM and the main signaling pathways controlling cell survival or death depending upon growth factors availability. Moreover, we demonstrated that the survival of peripheral mononuclear cells from AD patients was also dependent on Ca^{2+}/CaM signaling [25]. This observation, together with the fact that similar changes were found in cell signaling molecules or cell cycle regulatory proteins in fresh isolated or EBV-immortalized lymphocytes from AD patients [17], indicates that cell responsiveness is not altered by transformation. The present work aimed at elucidating whether there is a distinct regulation of CaM levels in AD lymphoblasts. Calcium binding protein is encoded by three genes, *CALM1, 2,* and *3*, which are located on chromosome 2 (2p21.1-p21.3), 14 (14q24–31) and 19 (19q13.2–13.3) [27] respectively. We investigated the expression of these genes and protein levels, as well as determined the rate of CaM degradation in control and AD cells. In addition, we examined crosstalk between CaM and the PI3K/Akt signaling pathway in the stimulation of proliferation of peripheral cells from AD patients.

MATERIAL AND METHODS

Materials.

All components for cell culture were obtained from Invitrogen (Carlsbad, CA). Calmidazolium (CMZ), W-13, N-(4-aminobutyl)-5-chloro-1-naphthalene sulfonamide, ionomycin, BAPTA, GSH, trolox and the proteasome inhibitor lactacystin were obtained from Sigma Aldrich (Alcobendas, Spain). The caspase inhibitor benzyloxy-carbonyl-Val-Asp-fluoromethylketone (Z-VAD-Fmk) was obtained from Calbiochem (Darmstad, Germany). Poly (vinylidene) fluoride (PVDF) membranes for western blots were purchased from Bio-Rad (Richmond, CA). Rabbit polyclonal antibodies (pAbs) against human phospho-Akt (Ser473) and rabbit anti-total CaMKII were obtained from Cell Signaling (Beverly, MA) Mouse monoclonal antibody anti-human PI3K p85α (sc-1637) and pAbs such as rabbit anti-human CaM I (FL-149), rabbit anti-human Ub (FL-76), rabbit anti-human pCaMKII (Thr286) (sc-12886-R) and goat anti-human total-Akt (sc-1618) were from Santa Cruz Biotechnologies (Santa Cruz, CA). Rabbit anti-human ß-actin antibody was from Sigma. The enhanced chemiluminiscence (ECL) system was from Amersham (Uppsala, Sweden). All other reagents were of molecular grade.

Cell lines

A total of 20 patients diagnosed in the department of Neurology of the University Hospital Doce de Octubre (Madrid, Spain) of probable Alzheimer according to NINCDS-ADRDA (National Institute of Neurological and Communicative Diseases and Stroke-Alzheimer's Disease and Related Disorders Association) criteria were used in this study. The average age of onset of the disease was 74±2 years. A group of 20 non-demented age-matched individuals was used as control. The frequency of the ApoE 4 allele was found to be 3% in the control group and 39% in the AD group in agreement with values previously reported for the control and AD population of Spain [28], and consistent with the late-onset form of AD. In all cases peripheral blood samples were obtained after written informed consent of the patients or their relatives.

Establishment of lymphoblastic cell lines was performed in our laboratory as previously described by infecting peripheral blood lymphocytes with the Epstein Barr virus [29]. Cells were grown in suspension in T flasks in an upright position, in approximately 10 ml of RPMI-1640 (Gibco, BRL) medium that contained 2 mM L-glutamine, 100 mg/ml penicillin/streptomycin and, unless otherwise stated, 10 % (v/v) fetal bovine serum (FBS) and maintained in a humidified 5% CO_2 incubator at 37 ºC. Fluid was routinely

changed every two days by removing the medium above the settled cells and replacing it with an equal volume of fresh medium.

Determination of cell proliferation.

Proliferation was determined by cell counting in a Neubauer chamber. Potential toxicity of the reagents used was routinely checked by trypan blue exclusion under inverted phase-contrast microscopy.

Quantitative reverse transcription-PCR.

Total RNA was extracted from cell cultures using the Trizol™ reagent (Invitrogen). RNA yields were quantified spectrophotometrically and RNA quality was checked by the A260/A280 ratio and on a 1.2% agarose gel to observe the integrity of 18S and 28S rRNA. RNA was then treated with DNase I Amplification Grade (Invitrogen). One microgram was reverse transcribed with the Superscript III Reverse Transcriptase kit (Invitrogen). Quantitative real-time PCR was performed in triplicates using TaqMan Universal PCR MasterMix No Amperase UNG (Applied Biosystems) reagent according to the manufacturer's protocol. Primers were used at a final concentration of 20 μM. The sequences of the primers used for real time PCR are listed in Table 1.

Real time quantitative PCR was performed in the BioRad iQ5 system using a thermal profile of an initial 5-min melting step at 95ºC followed by 40 cycles at 95ºC for 10s and 60ºC for 60s.

Relative mRNA levels of the genes of interest were normalized to ß-actin expression using the simplified comparative threshold cycle delta *CT* method [$2^{-(\Delta CT\ CaM - \Delta CT\ Actin}$].

Measurement of free intracellular Ca^{2+}.

Intracellular Ca^{2+} levels were determined using the Fluo4-AM probe (Molecular Probes), which binds Ca^{2+} with a 1:1 stoichiometry. Control and AD lymphoblasts were incubated in RPMI medium containing 10% FBS for 24 h. Then, cells were harvested, washed once with PBS and resuspended in fresh buffer. The cells were then incubated in the dark with 1 μM Fluo4-AM for 30 min at 37ºC, and the fluorescence was measured at FL-1 (530 nm) in a flow cytometer (EPICS-XL cytofluorimeter (Coulter Científica, Móstoles, Spain)) with an excitation laser at 488 nm. At least 10,000 events per sample were acquired.

Measurement of Reactive Oxygen Species.

The intracellular accumulation of ROS was determined using the fluorescent probe CM-H_2DCFDA (Invitrogen, C6827). After treatment of AD lymphoblasts with the antioxidant agents for 24 hours the cells were collected by centrifugation, resuspended in PBS, and loaded with 10 μM CM-H_2DCFDA

during 30 min. Fluorescence measurements were carried out using a POLARstar Galaxy spectrofluorimeter (BMG Labtechnologies, Offenburg, Germany). The excitation wavelength was 495 nm and the emission wavelength was 510nM.

Immunological analysis.

Cell extracts. To prepare whole cell extracts, cells were harvested, washed in PBS and then lysed in ice-cold buffer (50 mM Tris pH 7.4, 150 mM NaCl, 50 mM NaF, 1% Nonidet P-40), containing 1 mM sodium orthovanadate, 1 mM PMSF, 1 mM sodium pyrophosphate and protease inhibitor Complete Mini Mixture (Roche, Mannhein).

The protein content of the extracts was determined by the Pierce BCA Protein Assay kit (Thermo Scientific, Rockford, IL, USA).

Western blot analysis.

50-100 μg of protein from whole cell extracts were fractionated on a SDS polyacrylamide gel, and transferred to PVDF membrane (BioRad, Hercules CA). The amount of protein and the integrity of transfer were verified by staining with Ponceau-S solution (Sigma). The filters were then blocked with 1-5% BSA and incubated, overnight at 4ºC, with primary antibodies at the following dilutions: 1:1000 anti-phospho Akt, 1:1000 anti-Akt, 1:5000 anti-β -actin, 1:500 anti-pCaMKII, 1:1000 anti-CaMKII, 1:500 anti-CaM, 1:500 anti-p85α, 1:500 anti-Ub. Signals from the primary antibodies were amplified using species-specific antisera conjugated with horseradish peroxidase (Sigma) and detected with a chemiluminiscent substrate detection system ECL (Amersham). The specificity of the antibodies, used in this work, was checked by omitting the primary antibodies in the incubation medium. Blots were stripped and reprobed with anti-ß-actin as a protein loading control. The relative protein levels were determined by scanning the bands with a GS-800 imaging densitometer provided with the Quantity One 4.3.1. software from BioRad, and normalized by that of ß-actin.

Co-immunoprecipitation assays.

For CaM/Ub experiments, lymphoblasts from control and AD individuals were seeded at an initial density of $1x10^6$ cells/ml and incubated for 6 hours in the absence or in the presence of 1μM MG132. Lysates were collected and 1 mg of protein extract was subjected to immunoprecipitation overnight at 4ºC with anti-CaM antibody. Samples were incubated with protein G Sepharose (GE Healthcare Bio-

Sciences) and the resultant immunoprecipitates were washed three times in ice-cold lysis buffer. The samples were then treated with protein sample buffer and boiled prior to immunoblotting. Western blotting was then performed using the indicated antibodies

For p85/CaM experiments, lymphoblasts from control and AD individuals were seeded at an initial cell density of 1 x 10^6 cells/ml and incubated for 24 h. Protein extracts (1 mg) were subjected to immunoprecipitation overnight at 4ºC with an anti-p85 monoclonal antibody in the presence of 0.1mM $CaCl_2$ or 2mM EGTA. Samples were incubated then with protein G Sepharose (GE Healthcare Bio-Sciences) for 2 h at 4ºC. Immunocomplexes were washed three times with ice-cold lysis buffer containing $CaCl_2$, 1 μM CMZ or 2 mM EGTA, suspended with sample buffer, boiled, resolved in SDS-polyacrylamide gel, and transferred onto PVDF transfer membrane filters. Blots were probed with an anti-CaM polyclonal antibody. Membranes were reprobed with the anti-p85 antibody to check for equal immunoprecipitation efficiency.

Statistical analysis.

Unless otherwise stated, all data represent means±SE. Statistical analysis was performed on the Data Desk package (version 4.0) for Macintosh. Statistical significance was estimated by the Student's t-test or, when appropriated, by analysis of variance (ANOVA) followed by the Fischer's LSD test for multiple comparisons. Differences were considered significant at a level of $p<0.05$.

RESULTS

CaM levels and proliferative activity of control and AD lymphoblasts.

Fig. 1A shows a comparative analysis of CaM content after 72 h of serum addition between control and AD lymphoblasts. It is shown that lymphoblasts from AD patients had increased levels of CaM compared with CaM content in control cells. In these conditions, lymphoblasts from AD patients showed higher rates of cell proliferation (Fig. 1B) in agreement with previous reports [16]. Treatment of cells with two, structurally unrelated, antagonists of CaM, such as calmidazolium (CMZ) or W13 [30, 31], abrogated the serum-enhanced proliferation of AD cells, without affecting the proliferative activity of control lymphoblasts (Fig. 1B).

Regulation of CaM levels.

Bearing in mind the apparent relevance of CaM for the enhanced proliferative response of AD lymphoblasts, we were interested in elucidating the mechanisms by which CaM levels are regulated. First, by using real time quantitative PCR, *CALM 1, 2*, and *3* mRNAs expression levels were determined in control and AD lymphoblasts and the results are shown in Table 2. No differences in CaM mRNA abundance were detected between control and AD cells. Therefore, the increased CaM protein content of AD lymphoblasts, had to be ascribed to a post-transcriptional event.

To test whether the higher CaM content of AD lymphoblasts was dependent on altered protein degradation, we evaluated the stability of the CaM protein, by treating control and AD cells with 20 μg/ml of cycloheximide to inhibit de novo protein synthesis. At the indicated time, steady-state levels of CaM were determined by immunoblotting (Fig. 2). It is shown that CaM disappeared faster in control than in AD cells. The half-life of CaM was estimated in 22.1 ± 4 h in AD lymphoblasts versus 6.1 ± 1.2 h in control cells. The decreased rates of CaM degradation in AD cells was not due to nonspecific impairment of general protein degradation since no differences were observed in the rate of degradation of β-actin between control and AD lymphoblasts (Fig. 2).

Differences in degradation of apo-form of CaM or Ca^{2+}-bound CaM had been reported [10]. For this reason we determined whether half-life of CaM could be influenced by alteration of intracellular Ca^{2+} levels. For these experiments, we incubated control cells with the ionophore, ionomycin, and AD cells with the intracellular Ca^{2+} chelator BAPTA to increase or decrease the respective intracellular Ca^{2+} levels. Fig. 3 shows how ionomycin decreased the rate of degradation of CaM in control cells. Conversely,

decreasing the intracellular Ca^{2+} content of AD lymphoblasts resulted in enhanced CaM degradation approaching a half-life value close of that of control cells (Fig. 3). Fig. 4 depicts the intracellular Ca^{2+} levels under these conditions. The relative cellular Ca^{2+} content was assessed by Fluo-4AM staining and flow cytomertry. As expected, the peak fluorescence was displaced to higher intensity values, indicating increased levels of intracellular Ca^{2+} in control cells treated with ionomycin (Fig. 4). On the other hand treatment of AD cells with BAPTA effectively decreased the intracellular levels of Ca^{2+}. Fig. 4B summarizes the comparison of peak fluorescence displacement in control and AD lymphoblasts in the absence or in the presence of ionomycin or BAPTA. In agreement with previous reports [14], the basal Ca^{2+} concentration of AD lymphoblasts was higher than that of control cells (Fig. 4B).

It has been suggested that cellular aging and degenerative diseases lead to increased generation of reactive oxygen species (ROS) and a decline in proteolytic activity, resulting in the progressive accumulation of oxidatively damaged proteins and cellular dysfunction [32]. For this reason, we found it interesting to elucidate whether treatment of AD lymphoblasts with the antioxidants GSH or trolox, modifies the rate of CaM degradation. Fig. 5A shows that both treatments decreased significantly the half-life of CaM in AD lymphoblasts. Fig. 5B shows that untreated AD cells had increased ROS levels than control cells, and the efficacy of either GSH or trolox in decreasing ROS generation up to levels found in control cells.

The degradation of the CaM protein is mainly proteasome-dependent.

To elucidate the involvement of the major pathways for protein turnover in CaM degradation, we used a battery of protease inhibitors with selective specificity. Data in Fig. 6A show that both in control and AD lymphoblasts, CaM accumulated only in the presence of the highly selective proteasome inhibitor lactacystin. In contrast, treatment of cells with the lysomotropic agents hydroxychloroquine, CH_3NH_2 or NH_4Cl had no effect on cellular CaM content (Fig. 6A). Similarly, the lack of effect of z-VAD-fmk ruled out the involvement of caspases on CaM degradation (Fig. 6A). None of these inhibitors increased the levels of ß-actin, which was used as control. Collectively, these results suggested a predominant role for the proteasome system on CaM proteolysis.

To investigate if CaM degradation was accompanied by ubiquinitation of the molecule, we incubated control and AD lymphoblasts in the absence or in the presence of the proteasome inhibitor MG132 to ensure that ubiquitinated CaM was accumulated. CaM was imnunoprecipitated from these cells extracts with the anti-CaM antibody and then probed for ubiquitin with the anti-Ub antibody (Fig. 6B). It is

shown that indeed CaM is ubiquitinated. Although small, it seems to be a decrease in CAM polyubiquitination in AD cells (Fig. 6B).

Ca^{2+}/CaM regulation of AD lymphoblasts activity

The upregulation of CaM protein levels in lymphoblasts from AD patients raises the question as to whether higher CaM levels are related with increased activity of Ca^{2+}/CaM targets in these cells lines. Fig. 7A shows, that indeed CaMKII was overactivated in AD cells as compared to control cells, and that the CaM antagonist CMZ prevented CaMKII autophosphorylation. Similarly, PI3K/Akt activity, monitored by Akt phosphorylation, is enhanced in AD lymphoblasts (Fig. 7B). The overactivation was prevented by the CaM antagonists CMZ and W-13, but not with the CaMKII inhibitor KN-62, indicating that CaM-induced activation of PI3K/Akt was not mediated by this CaM-dependent kinase. These inhibitors didn't change basal levels of PI3K activity in control cells, suggesting the existence a threshold for CaM activation. Since the p85 regulatory subunit of PI3K/Akt had been shown to bind CaM [33, 34], we investigated whether the enhanced PI3K/Akt activity in AD lymphoblasts was due to differences in the CaM-p85 interaction between control and AD cells. To this end, cell lysates from control and AD lymphoblasts were immunoprecipitated with the anti-p85 antibody. The immunoprecipitates were resolved by SDS-PAGE, and the immunoblots were probed with an anti-CaM antibody. Clearly, CaM was found to co-immunoprecipitate with p85 in AD extracts (Fig. 8). Immunocomplexes formation was scarce in control extracts (Fig. 8). As previously described [34], CaM and p85 interaction was found to be Ca^{2+}-dependent (Fig. 8). When CMZ or W-13 was added during the immunoprecipitation process the association was strongly reduced (Fig. 8). These results suggest that treatment of AD cells with CaM antagonists could prevent CaM-mediated overactivation of PI3K, and therefore overcome the enhanced proliferative activity of AD lymphoblasts [17].

DISCUSSION

Previous work from our laboratory indicated impaired Ca^{2+}/CaM-dependent signaling in immortalized lymphocytes from AD patients, resulting in increased proliferative activity upon serum stimulation, and higher resistance to serum deprivation-induced apoptosis [16, 17, 25]. The present work was undertaken to evaluate whether the regulation of CaM content was altered in lymphoblastoid cell lines from late-onset AD patients. These cell lines, easily accessible, had previously proved to be useful model to study cell cycle-related events associated to neurodegeneration [16, 35]. Three major conclusions can be drawn from our work: first, CaM levels are increased in AD lymphoblasts; second, CaM half-life is enhanced in AD cells, and third, the rate of CaM degradation is dependent on intracellular Ca^{2+} levels and ROS status of the cell.

Increased levels of CaM were associated with overactivation of PI3K/Akt and enhanced proliferation of AD cells. These results are in line with the known role of CaM in regulating cell cycle progression [22]. In addition, both processes were sensitive to CaM antagonists, although these compounds were not able to decrease proliferation or PI3K/Akt activity in control cells [17], indicating the existence of a threshold of CaM dependent activation of PI3K/Akt and cell proliferation.

Our results suggested that the increased CaM levels in AD cells synergize with serum to overactivate PI3K/Akt pathway. In agreement with previous reports [33, 34] we found that CaM is able to bind to the 85 KDa regulatory subunit of PI3K (p85). Moreover it was observed a significant higher binding of CaM to p85 in AD lymphoblasts compared to control cells, thereby resulting in enhanced Akt phosphorylation.

The up-regulation of CaM levels in AD lymphoblasts is not the consequence of altered expression of any of the three different genes that encode CaM, but rather the result of decreased rates of CaM degradation. The half-life of CaM in AD lymphoblasts was estimated in 22 h, approximately 3 times fold of that of control cells. These values are in consonance with the reported half-life of CaM in rat brain [36]. It is worth to highlight that CaM has a very much shorter half-life than other calcium homeostasis related enzymes, such as plasma membrane Ca-ATPase (12 days) in the same tissue, but resembles the half-life of the bulk of cell proteins [36].

CaM exhibited proteasome-sensitive turnover. CaM accumulated when control or AD cells were treated with lactacystin, while CaM content was not affected by either caspase or autophagy inhibitors. The proteasomal degradation of CaM was accompanied by ubiquitination of the molecule, as co-immunoprecipitation of ubiquitin and CaM was observed in cell extracts from control and AD lymphoblasts. Apparently there is a slight decrease in the polyubiquitation of CaM in AD cells, which may contribute to the reduced CAM degradation in these cell lines. However, it was reported that aged or oxidized CaM can be efficiently degraded by either the 20S or 26S

proteasome in an ubiquitin-independent manner [10, 37]. More likely, both ubiquitin-dependent and independent mechanisms of proteasome degradation of CaM can operate *in vivo*. Further work is needed to clarify this point and to evaluate their potential contribution to CaM levels regulation.

Work from our and other laboratories demonstrated no global proteasome activity deficiency in lymphocytes from AD patients [17, 38, 39]. Indeed we reported enhanced proteasome-dependent degradation of the CDK inhibitor p27 in AD lymphoblasts [17]. On the other hand, the rate of β-actin degradation is similar in both control and AD lymphoblasts. Thus, the decreased rate of CaM degradation cannot be the result of nonspecific impairment of protein degradation in lymphoblasts from AD patients.

Intracellular Ca^{2+} levels and oxygen reactive species content appear to regulate the rate of CaM degradation in immortalized lymphocytes. Buffering the intracellular Ca^{2+} increase by BAPTA, restored the normal rate of CaM degradation. Conversely, treatment of control cells with ionomycin increased the CaM half-life in control cells. Reducing the rate of CaM degradation could be the cellular response to buffer Ca^{2+} overload. Previous work indicated that ubiquitination and degradation of CaM *in vitro* show opposite sensitivity to Ca^{2+} [10]. The rate of CaM degradation decreased in the presence of Ca^{2+}. It was suggested that ubiquitinated CaM could retain sufficient Ca^{2+} binding capacity to maintain a structure too rigid to be unfolded and directed to the proteasome [10]. On the other hand, treatment with antioxidants also normalized CaM degradation in AD lymphoblasts. It is known that enhanced ROS generation perturbs Ca^{2+} fluxes [40]. Thus, the effect of ROS controlling the rate of CaM degradation may play an additional role in ROS-induced disruption of Ca^{2+} homeostasis.

Despite the increased levels of CaM, AD lymphoblasts showed elevated intracellular concentration of Ca^{2+} in agreement with reports showing diminished Ca^{2+} buffering capacity in lymphoblasts from late-onset AD patients [14]. Moreover, decreased Ca^{2+} binding proteins in AD brain had also been reported [41]. These observations together with altered Ca^{2+} fluxes may contribute to the increased cytosolic Ca^{2+} of AD cells [42].

The binding of up to four calcium ions to CaM elicits significant conformational changes that increase the exposure of hydrophobic residues, e.g., Met, that serve as binding sites for target proteins [4]. In addition, the extent of Ca^{2+} saturation and location of bound Ca^{2+} ions within the CaM molecule also influence CaM's binding to targets [43]. As already mentioned we observed enhanced binding of CaM with the p85 regulatory subunit of PI3K in AD lymphoblasts. The activity of PI3K, as assessed by monitoring Akt phosphorylation, was also enhanced in AD lymphoblasts and sensitive to CaM antagonists. The activity of other CaM-dependent protein, CAMKII, was also found to increase in lymphoblasts from AD patients. This protein plays an important role in controlling the cellular response to serum-deprivation-induced apoptosis in immortalized lymphocytes [25, 26].

Despite the role of Ca^{2+}/CaM signaling in AD pathology, the mechanisms controlling CaM levels have received little attention. The increased CaM content of AD lymphoblasts reported here contrasts with previously reported reduction of CaM in AD-affected cerebral cortex [44]. The discrepancy may be due to differences in the ability of some anti-CAM antibodies to recognize CaM only in certain conformational states. Overactivation of PI3K/Akt has been, however, reported in AD brain. Increased posphorylation of Akt was detected in AD brain [45]. Furthermore, overactivated Akt in AD brain is accompanied by increased phosphoryaltion of Akt substrates, such as GSK3 or mTOR, and decreased levels of the CDKi p27 [46]. In this regard it is worth mentioning the enhanced Ca^{2+}/CaM/PI3K/Akt-dependent degradation of p27 previously reported in AD lymphoblasts [17]. Similarly, impaired CaMKII activation has been also detected in AD brain, associated with increased phosphorylation of tau and neurofibrillary tangle formation [47]. Thus, our results obtained in peripheral, easily accessible cells from AD patients, suggest that CaM degradation may also be perturbed in AD brain. Altered CaM levels in AD brain could play a role in the cell cycle disturbances-induced neuronal apoptosis. Therefore, the systemic failure of mechanism involved in CaM degradation, and thus of Ca^{2+}/CaM-dependent signaling pathways may be important to unravel the pathomechanism of AD.

COMPETING INTERESTS

The authors declare that they have no competing interests.

ACKNOWLEDGMENTS AND FUNDING

This work has been supported by grants from Ministry of Education and Science (SAF2007-62405, and SAF2010-15700) and Fundación Eugenio Rodríguez Pascual. NE holds a fellowship of the JAE predoctoral program of the CSIC.

REFERENCES

[1] Khachaturian ZS. Calcium hypothesis of Alzheimer's disease and brain aging. Ann N Y Acad Sci 747: 1-11 (1994).

[2] LaFerla FM. Calcium dyshomeostasis and intracellular signalling in Alzheimer's disease. Nat Rev Neurosci 3: 862-72 (2002).

[3] Mattson MP, Chan SL. Dysregulation of cellular calcium homeostasis in Alzheimer's disease: bad genes and bad habits. J Mol Neurosci 17: 205-24 (2001).

[4] Yamniuk AP, Vogel HJ. Calmodulin's flexibility allows for promiscuity in its interactions with target proteins and peptides. Mol Biotechnol 27: 33-57 (2004).

[5] O'Day DH, Myre MA. Calmodulin-binding domains in Alzheimer's disease proteins: extending the calcium hypothesis. Biochem Biophys Res Commun 320: 1051-4 (2004).

[6] Babu YS, Bugg CE, Cook WJ. Structure of calmodulin refined at 2.2 A resolution. J Mol Biol 204: 191-204 (1988).

[7] Babu YS*, et al.* Three-dimensional structure of calmodulin. Nature 315: 37-40 (1985).

[8] Kuboniwa H*, et al.* Solution structure of calcium-free calmodulin. Nat Struct Biol 2: 768-76 (1995).

[9] Zhang M, Tanaka T, Ikura M. Calcium-induced conformational transition revealed by the solution structure of apo calmodulin. Nat Struct Biol 2: 758-67 (1995).

[10] Tarcsa E, Szymanska G, Lecker S, O'Connor CM, Goldberg AL. Ca2+-free calmodulin and calmodulin damaged by in vitro aging are selectively degraded by 26 S proteasomes without ubiquitination. J Biol Chem 275: 20295-301 (2000).

[11] Persechini A, Stemmer PM. Calmodulin is a limiting factor in the cell. Trends Cardiovasc Med 12: 32-7 (2002).

[12] Tran QK, Black DJ, Persechini A. Intracellular coupling via limiting calmodulin. J Biol Chem 278: 24247-50 (2003).

[13] Eckert A, Forstl H, Zerfass R, Hennerici M, Muller WE. Free intracellular calcium in peripheral cells in Alzheimer's disease. Neurobiol Aging 18: 281-4 (1997).

[14] Ibarreta D, Parrilla R, Ayuso MS. Altered Ca2+ homeostasis in lymphoblasts from patients with late-onset Alzheimer disease. Alzheimer Dis Assoc Disord 11: 220-7 (1997).

[15] Li D*, et al.* Mutations of presenilin genes in dilated cardiomyopathy and heart failure. Am J Hum Genet 79: 1030-9 (2006).

[16] de las Cuevas N*, et al.* Ca2+/calmodulin-dependent modulation of cell cycle elements pRb and p27kip1 involved in the enhanced proliferation of lymphoblasts from patients with Alzheimer dementia. Neurobiol Dis 13: 254-63 (2003).

[17] Munoz U, Bartolome F, Bermejo F, Martin-Requero A. Enhanced proteasome-dependent degradation of the CDK inhibitor p27(kip1) in immortalized lymphocytes from Alzheimer's dementia patients. Neurobiol Aging 29: 1474-84 (2008).

[18] Lee HG*, et al.* Cell cycle re-entry mediated neurodegeneration and its treatment role in the pathogenesis of Alzheimer's disease. Neurochem Int 54: 84-8 (2009).

[19] McShea A*, et al.* Neuronal cell cycle re-entry mediates Alzheimer disease-type changes. Biochim Biophys Acta 1772: 467-72 (2007).

[20] Mosch B*, et al.* Aneuploidy and DNA replication in the normal human brain and Alzheimer's disease. J Neurosci 27: 6859-67 (2007).

[21] Davidkova G, Zhang SP, Nichols RA, Weiss B. Reduced level of calmodulin in PC12 cells induced by stable expression of calmodulin antisense RNA inhibits cell proliferation and induces neurite outgrowth. Neuroscience 75: 1003-19 (1996).

[22] Rasmussen CD, Means AR. Calmodulin is involved in regulation of cell proliferation. Embo J 6: 3961-8 (1987).

[23] Braunewell KH, Gundelfinger ED. Intracellular neuronal calcium sensor proteins: a family of EF-hand calcium-binding proteins in search of a function. Cell Tissue Res 295: 1-12 (1999).

[24] Nixon RA*, et al.* Calcium-activated neutral proteinase (calpain) system in aging and Alzheimer's disease. Ann N Y Acad Sci 747: 77-91 (1994).

[25] Bartolome F, de Las Cuevas N, Munoz U, Bermejo F, Martin-Requero A. Impaired apoptosis in lymphoblasts from Alzheimer's disease patients: cross-talk of Ca2+/calmodulin and ERK1/2 signaling pathways. Cell Mol Life Sci 64: 1437-48 (2007).

[26] Bartolome F*, et al.* Simvastatin overcomes the resistance to serum withdrawal-induced apoptosis of lymphocytes from Alzheimer's disease patients. Cell Mol Life Sci 64 4257-4268 (2010).

[27] Berchtold MW, Egli R, Rhyner JA, Hameister H, Strehler EE. Localization of the human bona fide calmodulin genes CALM1, CALM2, and CALM3 to chromosomes 14q24-q31, 2p21.1-p21.3, and 19q13.2-q13.3. Genomics 16: 461-5 (1993).

[28] Ibarreta D, Gomez-Isla T, Portera-Sanchez A, Parrilla R, Ayuso MS. Apolipoprotein E genotype in Spanish patients of Alzheimer's or Parkinson's disease. J Neurol Sci 134: 146-9 (1995).

[29] Koistinen P. Human peripheral blood and bone marrow cell separation using density gradient centrifugation on Lymphoprep and Percoll in haematological diseases. Scand J Clin Lab Invest 47: 709-14 (1987).

[30] Chafouleas JG, Lagace L, Bolton WE, Boyd AE, 3rd, Means AR. Changes in calmodulin and its mRNA accompany reentry of quiescent (G0) cells into the cell cycle. Cell 36: 73-81 (1984).

[31] Gietzen K. Comparison of the calmodulin antagonists compound 48/80 and calmidazolium. Biochem J 216: 611-6 (1983).

[32] Davies KJ, Shringarpure R. Preferential degradation of oxidized proteins by the 20S proteasome may be inhibited in aging and in inflammatory neuromuscular diseases. Neurology 66: S93-6 (2006).

[33] Joyal JL*, et al.* Calmodulin activates phosphatidylinositol 3-kinase. J Biol Chem 272: 28183-6 (1997).

[34] Perez-Garcia MJ*, et al.* Glial cell line-derived neurotrophic factor increases intracellular calcium concentration. Role of calcium/calmodulin in the activation of the phosphatidylinositol 3-kinase pathway. J Biol Chem 279: 6132-42 (2004).

[35] de las Cuevas N, Munoz U, Hermida OG, Martin-Requero A. Altered transcriptional regulators in response to serum in immortalized lymphocytes from Alzheimer's disease patients. Neurobiol Aging 26: 615-24 (2005).

[36] Ferrington DA, Krainev AG, Bigelow DJ. Altered turnover of calcium regulatory proteins of the sarcoplasmic reticulum in aged skeletal muscle. J Biol Chem 273: 5885-91 (1998).

[37] Balog EM, Lockamy EL, Thomas DD, Ferrington DA. Site-specific methionine oxidation initiates calmodulin degradation by the 20S proteasome. Biochemistry 48: 3005-16 (2009).

[38] Blandini F*, et al.* Peripheral proteasome and caspase activity in Parkinson disease and Alzheimer disease. Neurology 66: 529-34 (2006).

[39] Ullrich C, Mlekusch R, Kuschnig A, Marksteiner J, Humpel C. Ubiquitin enzymes, ubiquitin and proteasome activity in blood mononuclear cells of MCI, Alzheimer and Parkinson patients. Curr Alzheimer Res 7: 549-55 (2010).

[40] Peng TI, Jou MJ. Oxidative stress caused by mitochondrial calcium overload. Ann N Y Acad Sci 1201: 183-8 (2010).

[41] Palop JJ*, et al.* Neuronal depletion of calcium-dependent proteins in the dentate gyrus is tightly linked to Alzheimer's disease-related cognitive deficits. Proc Natl Acad Sci U S A 100: 9572-7 (2003).

[42] Berridge MJ. Calcium hypothesis of Alzheimer's disease. Pflugers Arch 459: 441-9 (2010).

[43] Schumacher MA, Rivard AF, Bachinger HP, Adelman JP. Structure of the gating domain of a Ca2+-activated K+ channel complexed with Ca2+/calmodulin. Nature 410: 1120-4 (2001).

[44] Solomon B, Koppel R, Jossiphov J. Immunostaining of calmodulin and aluminium in Alzheimer's disease-affected brains. Brain Res Bull 55: 253-6 (2001).

[45] Rickle A*, et al.* Akt activity in Alzheimer's disease and other neurodegenerative disorders. Neuroreport 15: 955-9 (2004).

[46] Griffin RJ*, et al.* Activation of Akt/PKB, increased phosphorylation of Akt substrates and loss and altered distribution of Akt and PTEN are features of Alzheimer's disease pathology. J Neurochem 93: 105-17 (2005).

[47] McKee AC, Kosik KS, Kennedy MB, Kowall NW. Hippocampal neurons predisposed to neurofibrillary tangle formation are enriched in type II calcium/calmodulin-dependent protein kinase. J Neuropathol Exp Neurol 49: 49-63 (1990).

LEGENDS TO THE FIGURES

Fig. 1

Calmodulin levels and proliferative activity of control and AD lymphoblasts.

A: Immortalized lymphoblasts from control and AD individuals were seeded at an initial density of 1 x 10^6 x ml^{-1} and cultured for three days in RPMI medium containing 10% FBS. CaM was detected by immunoblotting. Band intensity was measured and normalized by that of β-actin. Values shown are the mean±standard error for 11 independent determinations carried out with cell lines derived from different control and AD individuals. Statistical significance was determined by the t test *$p<0.05$. B: Control and AD lymphoblasts were incubated as above in the absence or in the presence of 1μM CMZ or 10μM W-13 for three days. Everyday thereafter, cells were enumerated. Values shown are the mean ± S for at least six observations carried out with different cell lines from control or AD individuals. Statistical significance was determined by the t test *$p<0.05$.

Fig. 2

Half-life of CaM in control and AD lymphoblasts

Cells were serum-deprived and then stimulated by adding 10% FBS. At this moment cycloheximide (20μg/ml) was added. Cells were harvested 4, 8, and 24 h thereafter and CaM was detected by immunoblotting. Blots from a representative experiment are shown. The decay of the CaM signal was graphed as a function of time post-cycloheximide addition. Curves were fitted to calculate the half-lives of the proteins, using data from different experiments carried out with of cell lines derived from six control and six AD subjects.

Fig. 3

Influence of intracellular Ca^{2+} levels on the rate of CaM degradatiom.

A: Immortalized lymphoblasts from control individuals were seeded at an initial density of 1 x 10^6 x ml^{-1} and serum-deprived for 24 h. Cells were preincubated for 30 minutes in the presence of 1μM ionomycin and stimulated by adding 10%FBS. Then, cycloheximide (20μg/ml) was added. Cells were harvested 4, 8, and 24 h thereafter and CaM was detected by immunoblotting. The experiment was repeated obtaining similar results. B: AD lymphoblasts were incubated as above in the presence of the intracellular Ca^{2+} chelator BAPTA at a final concentration of 30μM. A representative immunoblot is shown. The decay of the CaM signal was graphed as a function of time post-cycloheximide addition. Curves were fitted to calculate the half-lives of the proteins, using

data from independent experiments carried out with four cell lines derived from AD individuals.

Fig. 4

Intracellular Ca^{2+} levels in control and AD lymphoblasts treated with ionomycin or BAPTA.

Control and AD lymphoblasts were incubated with 1μM ionomycin and 30μM BAPTA respectively for 24 hours as described in the legend to Fig. 3. Intracellular Ca^{2+} levels were then measured with the fluorescent probe Fluo4-AM. The upper plot shows peak displacement to higher or lower fluorescence in the presence of ionomycin or BAPTA respectively. Below, it is shown the relative mean fluorescence intensity ± SE, for at least six observations carried out in cell lines derived from different individuals.

Fig. 5

Effects of antioxidants on the rate of CaM degradation and ROS generation.

A: Serum-deprived lymphoblasts from AD patients were preincubated for 30min in the absence or in the presence of 10mM GSH or 1mM Trolox, and then stimulated by adding 10%FBS. Afterwards, cycloheximide (20μg/ml) was added. Cells were harvested 4, 8, and 24h thereafter and CaM was detected by immunoblotting. Results shown are the mean ± SE for at least 3 experiments carried out with different cell lines. B: Lymphoblasts from AD patients were incubated for 24 h in the absence or in the presence of 10mM GSH and 1mM Trolox. The intracellular ROS levels were determined in control and AD lymphoblasts with the fluoresecent probe CM-H_2DFCDA. Values shown are the mean ± SE for independent determinations carried out with eight different cell lines derived from control or AD individuals. *$p<0.05$ significantly different from control cells. **$p<0.05$ significantly different from AD cells without antioxidant treatment.

Fig. 6

CaM degradation appears to occur in the proteasome

A: Control and AD lymphoblasts were incubated for 24 h in the presence of the proteasome inhibitor lactacystin (L) (15μM), the caspase inhibitor z-VAD-fmk (Z) (50μM) or the autophagy inhibitors, hydroxychloroquine (H) (250μM); CH_3NH_2 (C) (15mM) or NH_4Cl (N) (15mM). CaM accumulated only in the presence of lactacystin. Values shown are the mean ± SE for 6-8 determinations carried out with cell lines derived from different individuals. B: Control and AD lymphoblasts were incubated for 24 h in the absence or in the presence of presence of the proteasome inhibitor MG132 (1μM). Lysates from these cell cultures were immunoprecipitated with anti-CaM antibody and probed for ubiquitin with the anti-Ub antibody. Efficiency of the

immunoprecipitation procedure was checked by reprobing the membranes using the anti-CaM antibody. The experiment was repeated once obtaining similar results.

Fig. 7

CaMKII and PI3K/Akt activities in control and AD lymphoblasts.

A: Immortalized lymphoblasts from control and AD patients were seeded at an initial density of 1 x 10^6 x ml^{-1} and cultured for 24 h in the absence or in the presence of the CaM antagonists CMZ (1mM) or the CaMKII inhibitor KN-62 (1μM). Whole cell lysates were immunoblotted with antibodies anti-phospho-CaMKII (Ser286) and total CaMKII. The densitometric data represents the mean ± SE for three independent determinations carried out with different cell lines *$p<0.05$ significantly different from control cells. **$p<0.05$ significantly different from AD cells incubated without inhibitors. B: Control and AD lymphoblasts were incubated as above in the absence or in the presence 1 μM CMZ, 10μM W-13 or 1μM KN-62. Phospho-Akt (Ser473) and total Akt were determined by immunoblotting. Representative immunoblots are presented. The densitometric data below represents the mean ± SE for determinations carried out with six different control and AD cell lines. *$p<0.01$ significantly different from control cells. **$p<0.01$ significantly different from AD cells incubated without inhibitors

Fig. 8

Effects of Ca^{2+} levels and calmodulin antagonists on CaM binding to p85 regulatory subunit of PI3K.

Lysates from control and AD lymphoblasts were immunoprecipitated with the anti-p85 antibody (α-p85) in the presence of 0.1 mM $CaCl_2$ or 2 mM EGTA, and 0.1 mM $CaCl_2$ plus 1μM CMZ or 10 μM W-13. Immunocomplexes were analyzed by Western blot with an anti-CaM antibody. Efficiency of p85 immunoprecipitation, in the different conditions, was checked by reprobing the membranes with the anti-α-p85 antibody. Representative experiments are shown. W-13 was used in two different experiments, while the effect of CMZ and EGTA was determined in four different immunoprecipitation experiments. Below it is presented the densitometric analysis. When present the bars represent the SE of the mean. *$p<0.01$, significantly different from control cells, **$p<0.01$ significantly different from AD cells incubated without inhibitors.

Table 1

Sequences of oligodeoxyribonucleotide primers used for quantitative real-time PCR

Gene	Primer sequence	
	Forward (5' → 3')	Reverse (5'→ 3')
CALM 1	AACAGAAGCTGAATTGCAGGA	AATTCGGGGAAGTCAATGG
CALM 2	ATGGCTGACCAACTGACTGA	CAGTTCCAATTCCTTTGTTG
CALM 3	AACCTTGATCCCCGTGCT	AGGCCTCCTTGAACTCTGC
β-ACTIN	CCAACCGCGAGAAGATGA	CCAGAGGCGTACAGGGATAG

Probes were designed using the Universal ProbeLibrary for Human (Roche Applied Science)

Table 2

Relative Calmodulin mRNA abundance

	CONTROL	AD
CALM 1	1 ± 0.109	1.12 ± 0.051
CALM 2	1 ± 0.183	0.86 ± 0,122
CALM 3	1 ± 0.123	1 ± 0.120

Immortalized lymphoblasts from control and AD individuals were seeded at an initial density of 1 x 10^6 x ml^{-1} and cultured for 3 days in RPMI medium containing 10% FBS. Cells were collected and subjected to RT-qPCR. Relative mRNA levels of the CaM genes were normalized to ß-actin expression, and values for control cells were set as one. Values shown are the mean ± SE for six different cell lines.

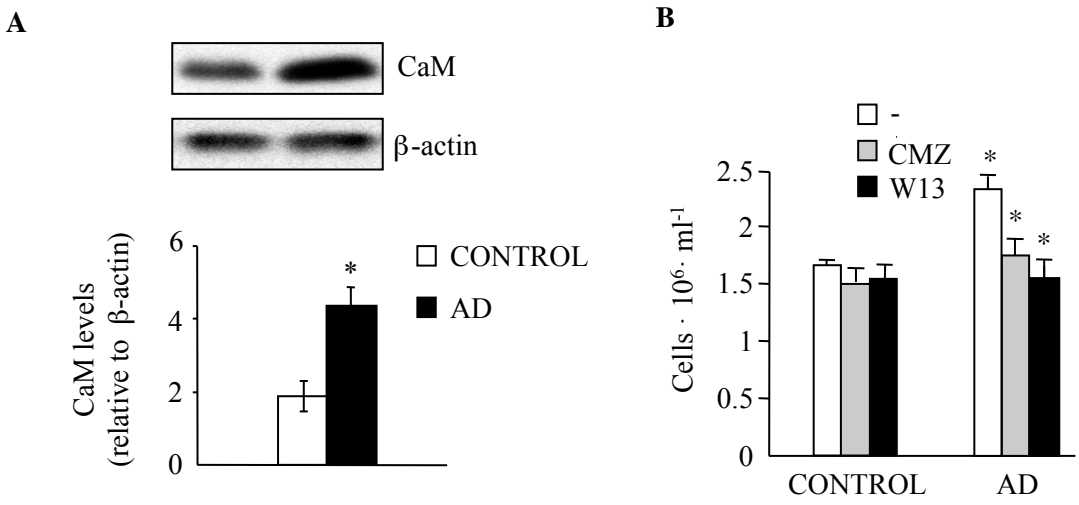
A
CaM
β-actin
CaM levels
(relative to β-actin)
6
4
2
0
*
CONTROL
AD
B
-
CMZ
W13
Cells · 10⁶ · ml⁻¹
2.5
2
1.5
1
0.5
0
*
*
*
CONTROL
AD

Fig. 1

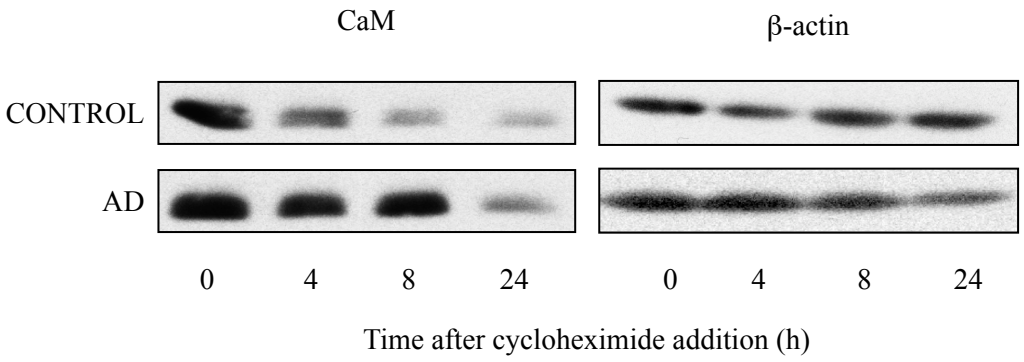
CaM
β-actin
CONTROL
AD
0
4
8
24
0
4
8
24
Time after cycloheximide addition (h)

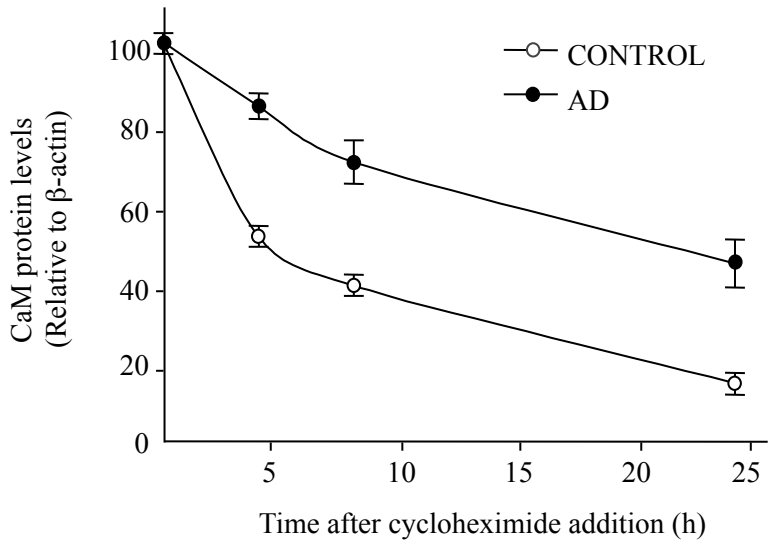
CONTROL
AD
CaM protein levels
(Relative to β-actin)
100
80
60
40
20
0
5
10
15
20
25
Time after cycloheximide addition (h)

Fig. 2

A

CONTROL

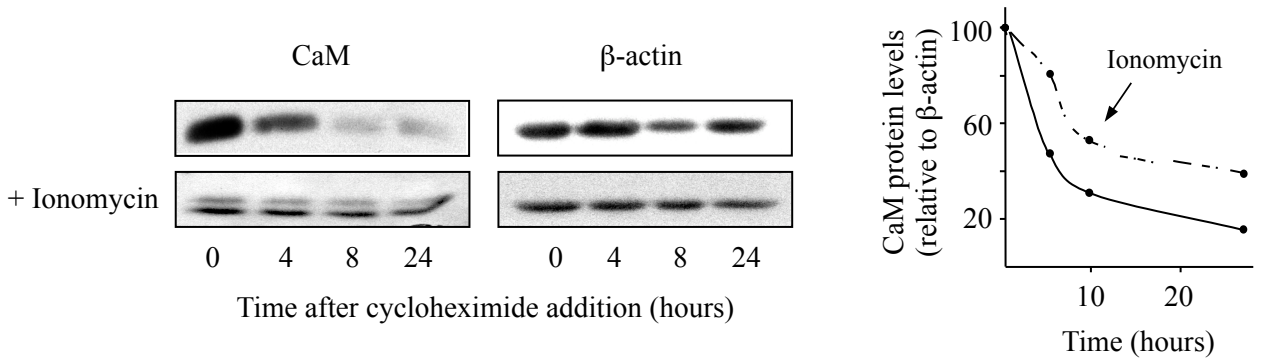

B

AD

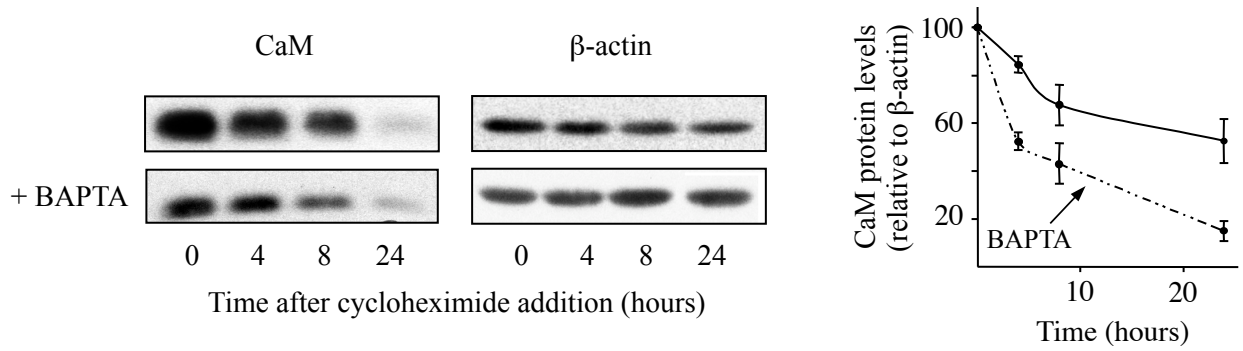

Fig. 3

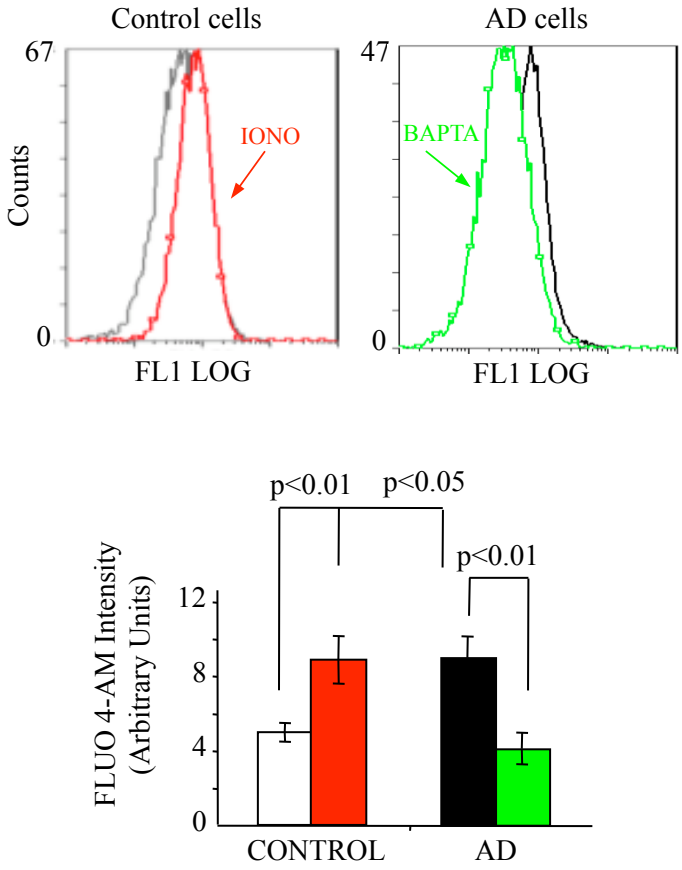
Control cells
AD cells
67
47
Counts
IONO
BAPTA
0
0
FL1 LOG
FL1 LOG
p<0.01
p<0.05
p<0.01
FLUO 4-AM Intensity
(Arbitrary Units)
12
8
4
0
CONTROL
AD

Fig. 4

A

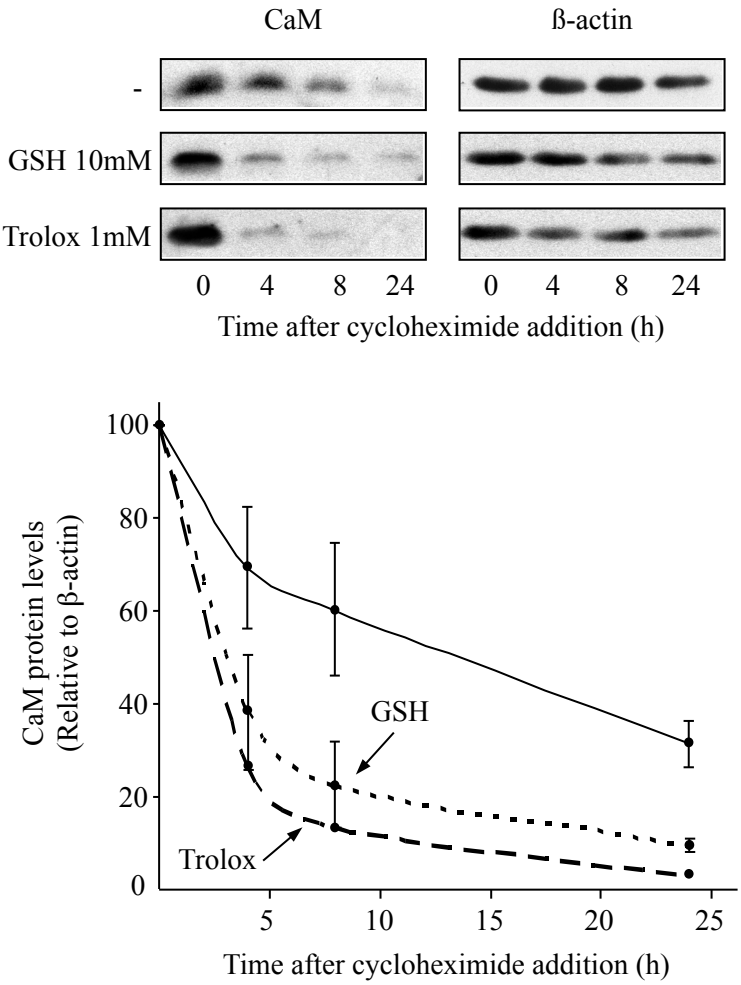
CaM
ß-actin
-
GSH 10mM
Trolox 1mM
0 4 8 24 0 4 8 24
Time after cycloheximide addition (h)
CaM protein levels
(Relative to β-actin)
100
80
60
40
20
0
GSH
Trolox
5 10 15 20 25
Time after cycloheximide addition (h)

B

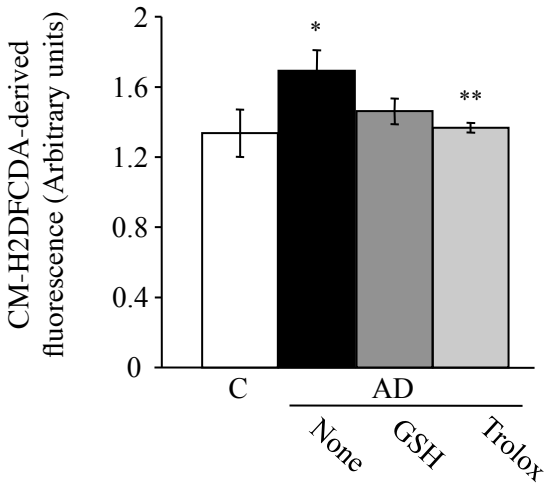
CM-H2DFCDA-derived
fluorescence (Arbitrary units)
2
1.6
1.2
0.8
0.4
0
*
**
C
AD
None
GSH
Trolox

Fig. 5

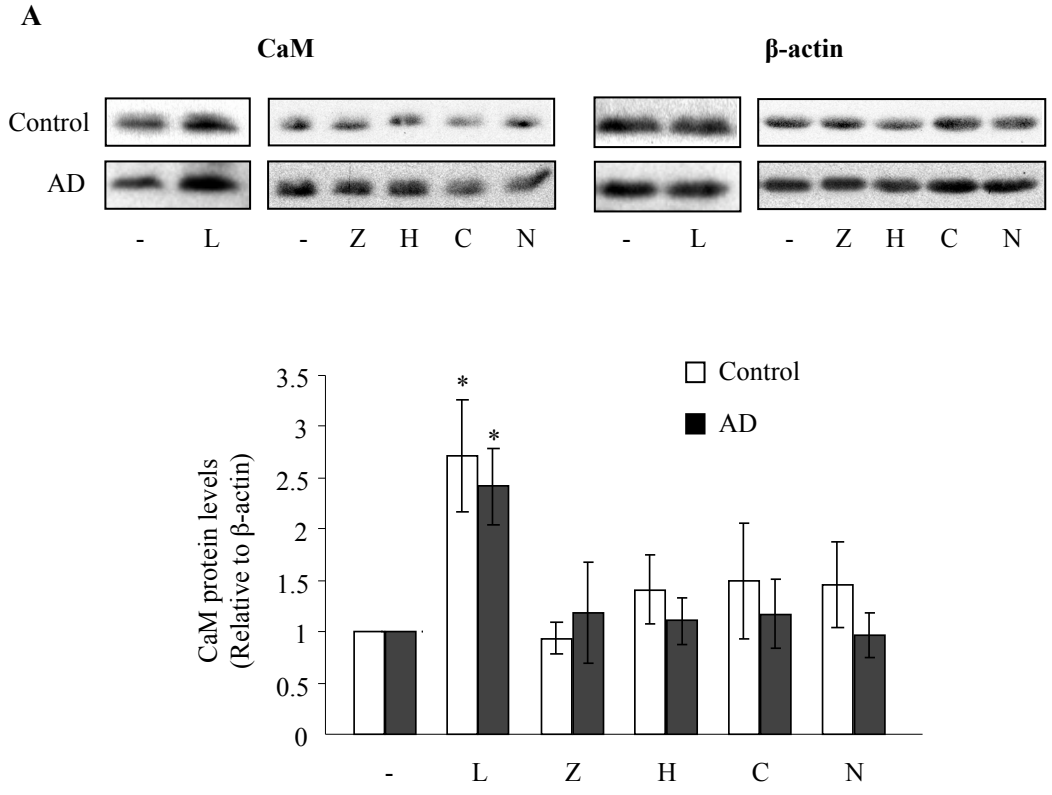
A
CaM
β-actin
Control
AD
- L - Z H C N - L - Z H C N
CaM protein levels (Relative to β-actin)
Control
AD
3.5
3
2.5
2
1.5
1
0.5
0
*
*
- L Z H C N

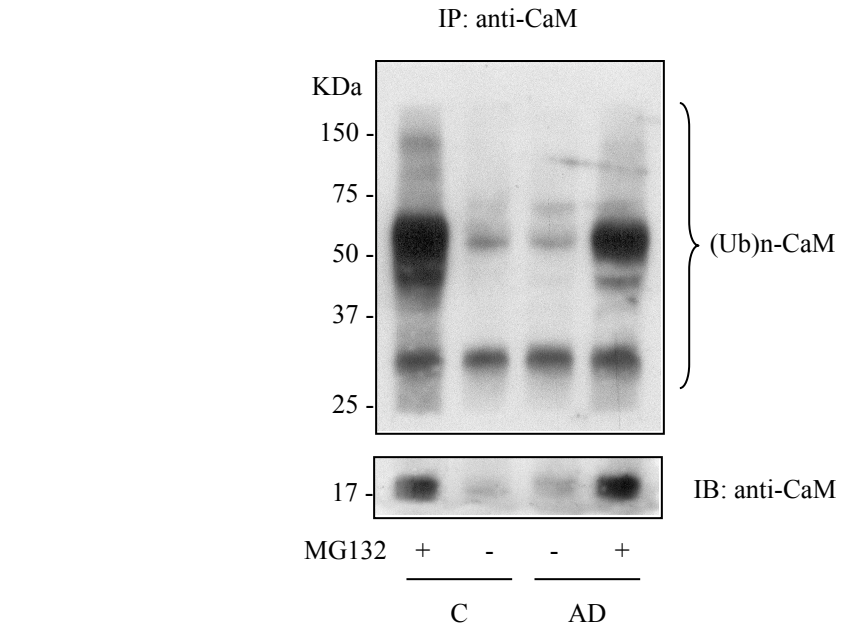
B
IP: anti-CaM
KDa
150
75
50
37
25
(Ub)n-CaM
17
IB: anti-CaM
MG132 + - - +
C
AD

Fig. 6

A

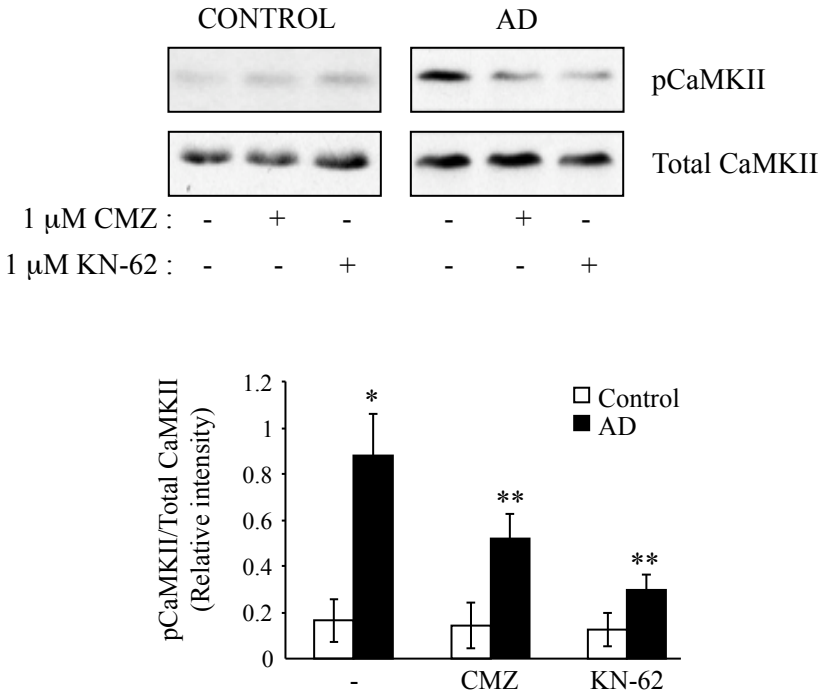
CONTROL
AD
pCaMKII
Total CaMKII
1 μM CMZ : - + - - + -
1 μM KN-62 : - - + - - +
pCaMKII/Total CaMKII (Relative intensity)
1.2
1
0.8
0.6
0.4
0.2
0
Control
AD
*
**
**
-
CMZ
KN-62

B

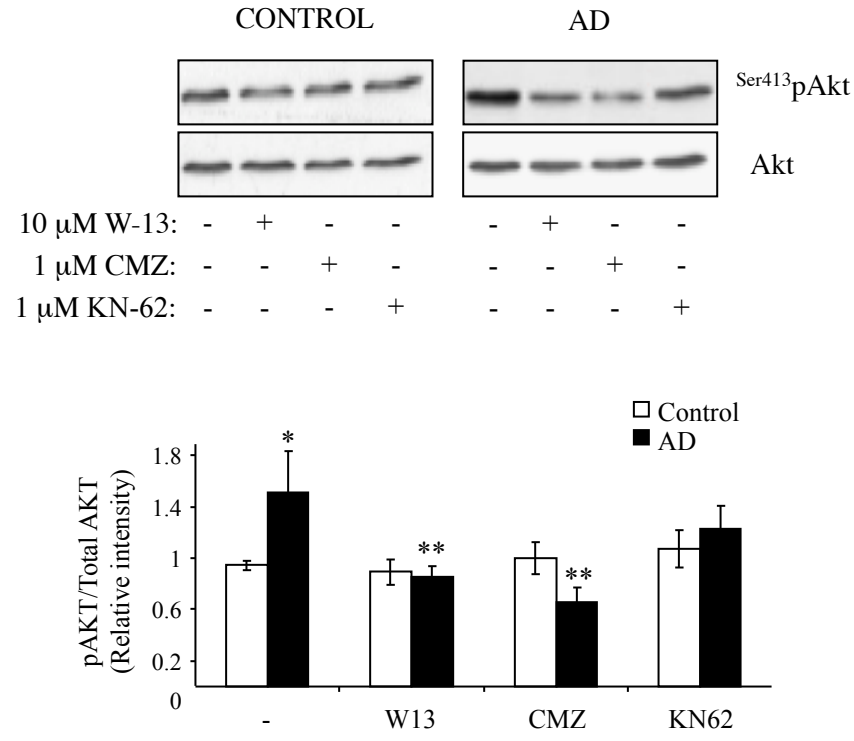
CONTROL
AD
Ser413pAkt
Akt
10 μM W-13: - + - - - + - -
1 μM CMZ: - - + - - - + -
1 μM KN-62: - - - + - - - +
pAKT/Total AKT (Relative intensity)
1.8
1.4
1
0.6
0.2
0
Control
AD
*
**
**
-
W13
CMZ
KN62

Fig. 7

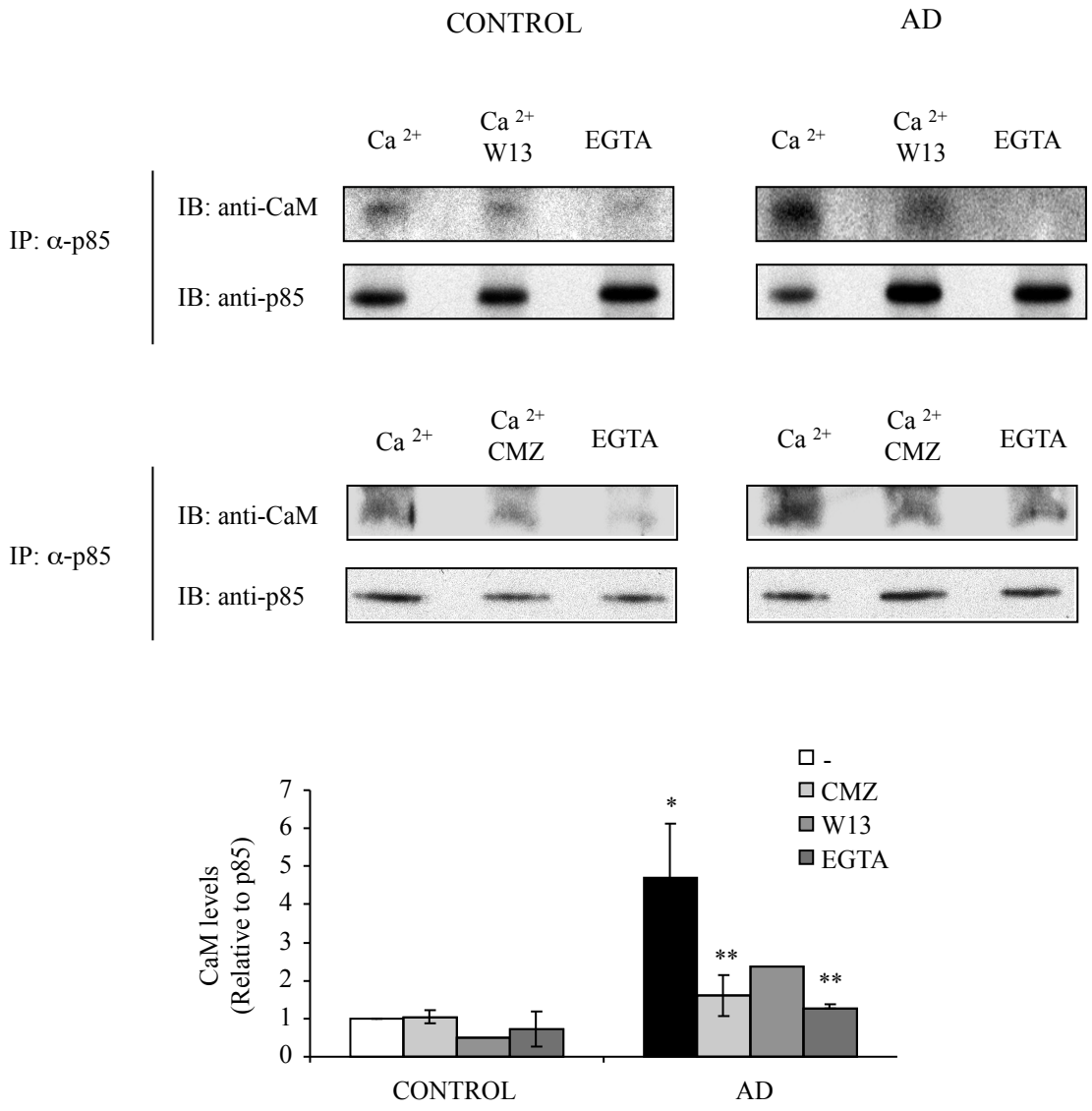
CONTROL
AD
Ca 2+
Ca 2+ W13
EGTA
IP: α-p85
IB: anti-CaM
IB: anti-p85
Ca 2+
Ca 2+ CMZ
EGTA
IP: α-p85
IB: anti-CaM
IB: anti-p85
CaM levels (Relative to p85)
0
1
2
3
4
5
6
7
*
**
**
-
CMZ
W13
EGTA
CONTROL
AD

Fig. 8